Androgen metabolite-dependent growth of hormone receptor-positive breast cancer as a possible aromatase inhibitor-resistance mechanism

Toru Hanamura[1,3], Toshifumi Niwa[1], Sayo Nishikawa[1], Hiromi Konno[1], Tatsuyuki Gohno[1], Chika Tazawa[1], Yasuhito Kobayashi[4], Masafumi Kurosumi[4], Hiroyuki Takei[5], Yuri Yamaguchi[6], Ken-ichi Ito[3], Shin-ichi Hayashi[1,2]

[1]Department of Molecular and Functional Dynamics, Graduate School of Medicine, Tohoku University, Sendai, Japan

[2]Center for Regulatory Epigenome and Diseases, Graduate School of Medicine, Tohoku University, Sendai, Japan

[3]Division of Breast and Endocrine Surgery, Department of Surgery, Shinshu University School of Medicine, Nagano, Japan

[4]Department of Pathology, Saitama Cancer Center, Saitama, Japan

[5]Division of Breast Surgery, Saitama Cancer Center, Saitama, Japan

[6]Research Institute for Clinical Oncology, Saitama Cancer Center, Saitama, Japan

Corresponding author: Shin-ichi Hayashi, Center for Regulatory Epigenomics and Diseases, Department of Molecular and Functional Dynamics, Graduate School of Medicine, Tohoku University, 2-1 Seiryo-machi, Aoba-ku, Sendai 980-8575, Japan.

Phone: +81-22-717-8680; Fax: +81-22-717-7913

e-mail: shin@med.tohoku.ac.jp

Abstract

Aromatase inhibitors (AIs) have been reported to exert their antiproliferative effects in postmenopausal women with hormone receptor-positive breast cancer not only by reducing estrogen production, but also by unmasking the inhibitory effects of androgens such as testosterone (TS) and dihydrotestosterone (DHT). However, the role of androgens in AI-resistance mechanisms is not sufficiently understood. 5α-Androstane-3β,17β-diol (3β-diol) generated from DHT by 3β-hydroxysteroid dehydrogenase type 1 (HSD3B1) shows androgenic and substantial estrogenic activities, representing a potential mechanism of AI resistance. Estrogen response element (ERE)-green fluorescent protein (GFP)-transfected MCF-7 breast cancer cells (E10 cells) were cultured for 3 months under steroid-depleted, TS-supplemented conditions. Among the surviving cells, two stable variants showing androgen metabolite-dependent ER activity were selected by monitoring GFP expression. We investigated the process of adaptation to androgen-abundant conditions and the role of androgens in AI-resistance mechanisms in these variant cell lines. The variant cell lines showed increased growth and induction of estrogen-responsive genes rather than androgen-responsive genes after stimulation with androgens or 3β-diol. Further analysis suggested that increased expression of HSD3B1 and reduced expression of androgen receptor (AR) promoted adaptation to androgen-abundant conditions, as indicated by the increased conversion of DHT into 3β-diol by HSD3B1 and AR signal reduction. Furthermore, in parental E10 cells, ectopic expression of HSD3B1 or inhibition of AR resulted in adaptation to androgen-abundant conditions. Coculture with stromal cells to mimic local estrogen production from androgens reduced cell sensitivity to AIs compared with parental E10 cells. These results suggest that increased expression of HSD3B1 and reduced expression of AR might reduce the sensitivity to AIs as demonstrated by enhanced androgen metabolite-induced ER activation and growth mechanisms. Androgen metabolite-dependent growth of breast cancer cells may therefore play a role in AI-resistance.

Keywords MCF-7 cell, Breast cancer, Aromatase inhibitor resistance, Androgen metabolism, Androgen receptor

Abbreviations

AI: aromatase inhibitor
TS: testosterone
DHT: dihydrotestosterone
3β-diol: 5α-androstane-3β,17β-diol
HSD3B1: 3β-hydroxysteroid dehydrogenase type 1
AKR1C3: aldo-keto reductase 1C3
AR: androgen receptor
ERα: estrogen receptor α
E2: estradiol
OHT: 4-hydroxytamoxifen
GFP: green fluorescent protein
SERM: selective estrogen receptor modulator

Introduction

The initial use of aromatase inhibitors (AIs) provides substantial clinical benefit in postmenopausal women with hormone receptor-positive breast cancer, compared with tamoxifen. Nevertheless, some patients still relapse [1, 2]. Postmenopause, estrogens are mainly derived by aromatase from androgens (testosterone (TS) and androstenedione) biosynthesized in the adrenal glands [3]. The generated estrogens can stimulate estrogen-dependent breast cancer growth in the absence of ovarian estrogens. Androgens, such as dihydrotestosterone (DHT) and its precursor TS, exert inhibitory effects in hormone-dependent breast cancer cells [4–6]. A previous study reported that the intratumoral estradiol (E2) concentration was 0.35-fold lower in breast carcinoma tissues from patients treated with exemestane, compared with those without therapy. In contrast, intratumoral DHT and TS concentrations were 2.3- and 1.6-fold higher, respectively, in breast carcinomas treated with exemestane, compared with those without exemestane therapy [7]. It has therefore been suggested that AIs may inhibit the growth of such tumors not only by blocking the conversion of adrenal androgens to estrogens [3, 8], but also by unmasking the inhibitory effect of androgens acting via the androgen receptor (AR) [9]. Previous reports have proposed several hypotheses to explain the mechanism responsible for AI resistance, including growth-signaling pathways independent of estrogen and estrogen receptor α (ERα) [10], and constitutive ERα activation caused by growth factor receptor pathways [11–13]. However, few studies have investigated the process of adaptation to androgen-abundant conditions or the role of androgens in AI-resistance mechanisms.

DHT is the most potent antiproliferative androgen for MCF-7 cells [9], and binds ARs with high affinity [14]. DHT can be metabolized to 5α-androstane-3β,17β-diol (3β-diol) by 3β-hydroxysteroid dehydrogenase type 1 (HSD3B1) and aldo-keto reductase 1C3 (AKR1C3) [15–17]. 3β-diol has been shown to bind not only ARs, but also ERα [18, 19], and to induce growth and activation of ERα under severely estrogen-deprived conditions, representing a potential mechanism of resistance to AIs [20]. However, the effects of AI treatment on androgen metabolism are not sufficiently understood. Furthermore, 3β-diol also has substantial binding affinity for AR [18], and the functions of androgen and 3β-diol in AI resistance remain unclear. We therefore investigated this issue using previously established estrogen response element (ERE)-green fluorescent protein (GFP)-transfected MCF-7 (E10 cells) [21, 22]. We successfully cloned two stable variant cell lines (V1 and V2 cells) that showed androgen metabolite-ER activity, by monitoring GFP expression. Using these variant cell lines, we investigated the processes of adaptation to estrogen-depleted and androgen-abundant conditions, and the role of androgens in AI-resistance mechanisms. We suggest that increased expression of HSD3B1 and reduced expression of AR might decrease the sensitivity to AIs, as indicated by enhancement of androgen metabolite-induced ER activation and cell growth.

Materials and methods

Reagents

E2, TS, DHT, 3β-diol, dexamethasone and 4-hydroxytamoxifen (OHT) were purchased from Sigma-Aldrich Inc. (St. Louis, MO, USA). Bicalutamide (AR inhibitor) was purchased from LKT Laboratories Inc. (St. Paul, MN, USA). Letrozole, exemestane and toremifene were kindly provided by Novartis Pharma K.K. (Tokyo, Japan), Pfizer Inc. (New York, NY, USA) and Nippon Kayaku Co. Ltd. (Tokyo, Japan), respectively.

Fulvestrant and anastrozole were kindly provided by Astra Zeneca K.K. (Osaka, Japan).

Cells and culture

E10 cells were established from the human breast cancer cell line MCF-7, as described previously [21, 22]. We analyzed ER transcriptional activity in individual living cells using GFP as a reporter gene (Online Resource 1, Fig. S1a). Stromal cells were isolated from breast cancer tissue as described previously [21]. E10 and stromal cells were cultured in RPMI1640 medium (Sigma-Aldrich) supplemented with 10% fetal calf serum (FCS; Tissue Culture Biologicals Inc., Tulare, CA, USA) as the regular growth medium at 37 °C in a humidified atmosphere of 5% CO_2 in air. Phenol red-free RPMI1640 (PRF-RPMI) (Gibco Brl, Grand Island, NY, USA) supplemented with 10% dextran-coated charcoal-treated FCS was used as steroid-depleted medium for each experiment.

Screening of variant cell lines

A schema of the screening method for the variant cell lines is shown in Fig. S1B (Online Resource 1). E10 cells were cultured for 3 months in steroid-depleted medium with 100 nM TS. Five colonies showing luminescence by GFP expression were selected and seeded separately. Further screening was carried out by assessing ER activities under the following treatments. The ER activity of each clone was measured based on the proportion of GFP-positive cells in culture (ERE-GFP assay). ER activity in steroid-depleted TS-supplemented cultures was initially measured (a), and the measurement was repeated after 3 days of culture in steroid-depleted medium (b) to exclude GFP-positive clones with constitutively-activated ER. TS 100 nM and 3β-diol 100 nM were added continuously to the culture medium and ER activity was confirmed at 24 h (c) to select the clones with a high affinity for the androgen metabolite. Finally, clones that retained ER activity even after the addition of 100 nM letrozole (d) were established, and named V1 and V2 cell lines. Simultaneously, ER activities in these cell lines were confirmed to be inhibited by 1 μM fulvestrant (e). These variant cell lines were maintained in steroid-depleted medium supplemented with 100 nM TS.

Cell growth assay

For assays under defined steroid hormone conditions, cells were washed and grown in steroid-depleted medium for 3 days, then plated in 24-well culture plates at a density of 10,000 cells/well in steroid-depleted medium. The cells were incubated for 4 days in the absence or presence of the tested drugs and hormones. The cells in each well were washed and harvested, and then counted using a Sysmex CDA-500 automated cell counter (Sysmex Corporation, Kobe, Japan).

ERE-luciferase reporter assays

ERE activity in each cell line was measured using the Dual-Luciferase Reporter Assay System (Promega, Madison, WI, USA). The estrogen reporter plasmid used, ERE-tk-Luci, has been described previously [23].

The vector pRL-TK (Promega) was used as an internal control of transfection efficiency in reporter assays. Transient transfection was performed as described previously [23]. After culturing the cells for a further 24 h in the absence or presence of the tested drugs and hormones, luciferase activity was measured using the Dual-Luciferase Reporter Assay System, according to the manufacturer's instructions.

Real-time polymerase chain reaction in cell lines

Total RNA was extracted from each cell line cultured in the indicated growth medium using Isogen (Nippon Gene Co., Ltd., Toyama, Japan), according to the manufacturer's instructions. The extracted RNA (1 μg) was converted to first-stranded cDNA primed with a random 9-mers in a 10-μL reaction volume using a Takara RNA PCR kit (AMV) Ver.3.0 (Takara Bio Inc. Otsu, Japan). A 2-μL aliquot was used as a template for real-time polymerase chain reaction (PCR).

Real-time PCR to detect expression of the indicated mRNA was carried out according to the manufacturer's standard protocol using an Applied Biosystems StepOne real-time PCR system (Life Technologies Japan, Tokyo, Japan). The expression of the target gene relative to RPL13A internal control was calculated. All PCRs were performed in duplicate, and the specificity of the reaction was determined by melting-curve analysis at the dissociation stage. Primer data and GenBank accession numbers of reference sequences are shown in Table S1 (Online Resource 2).

Establishment of HSD3B1 over-expressing E10 cells

Construction of the HSD3B1 expression vector and control vector was carried out as follows. The SV40 early promoter, blasticidin deaminase and SV40 poly(A) gene cassette was spliced out from the pMAM2-BSD vector (Kaken Chemicals Co., Tokyo, Japan) and inserted into the BamHI site of the pRL-CMV vector (Promega). The *Renilla* luciferase (Rluc) gene in the generated vector was then replaced with full-length HSD3B1 cDNA (HSD3B1 expression vector) or cut-off (control vector). The HSD3B1 expression vector or control vector was then transfected into E10 cells using TransIT LT-1 reagent (Mirus Co., Madison, WI, USA), following the manufacturer's protocol. Cells transfected with the HSD3B1 expression vector or control vector were selected using 10 mg/mL blasticidin. The expression levels of HSD3B1 were analyzed by real-time PCR (Online Resource 3, Fig. S2).

Cell growth and ERE-GFP reporter assays in coculture system

We were unable to assess the inhibitory effect of AIs in the E10 or variant cell lines because of their low aromatase expression. We therefore used cocultures, in which cancer cells and stromal cells were grown separated by a membrane, but interacted via soluble factors and shared the same microenvironment, including local estrogen synthesis from androgens by aromatase in stromal cells (Online Resource 4, Fig. S3).

All the cell lines were washed and grown in steroid-depleted medium for 3 days. Cancer cell lines were plated in the bottom well of 24-well culture plates at a density of 10,000 cells/well in steroid-depleted medium. Stromal cells were plated in the insert layer (0.4-μm pore cell-culture insert; Becton, Dickinson and

Company, Franklin Lakes, NJ, USA) at a density of 30,000 cells/well in steroid-depleted medium supplemented with 1 μM dexamethasone to enhance aromatase gene expression [21, 24]. The cells were then incubated for 4 days in the absence or presence of the tested drugs and hormones before being subjected to cell-growth and ERE-GFP reporter assays. Cancer cells in each bottom well were washed and harvested for cell counting and ERE-GFP assay.

Statistical analyses

Analyses of cell growth, and ERE-luciferase and ERE-GFP reporter assays were performed in triplicate. Data are presented as mean ± standard deviation (mean ± SD) except for the GFP assay for the establishment of variant cell lines. The Kruskal-Wallis test was used to compare three or more independent groups. The level of significance was set at $P < 0.05$.

Results

Selection of two variant cell lines showing androgen metabolite-dependent ER activity

After 3 months of culture in TS-supplemented steroid-depleted medium, five clones that retained ER activity were selected. The ER activities of these clones at each step are summarized in Fig. S1B and Fig. 1. Clones V4 and V5 retained ER activity in steroid-depleted conditions and were therefore considered to have constitutively-activated ER, by the growth factor receptor pathway or some other mechanism. ER activity in the V3 cell line was induced by TS and 3β-diol and suppressed by letrozole, suggesting that this ER activity depended on estrogens supplied by aromatase from TS, rather than 3β-diol. TS-induced ER activities in the V1 and V2 cell lines were inhibited by steroid depletion, and ER activities induced by TS and 3β-diol were higher than that induced by TS alone, and were not inhibited by letrozole. These results suggested that the V1 and V2 cell lines showed ER activity induced by androgen metabolites, with high affinities for the androgen metabolite. V1 and V2 were therefore defined as variant cell lines.

Androgens and 3β-diol showed estrogenic rather than androgenic function in variant cell lines

Dose-response curves for growth induced by TS, DHT, 3β-diol and E2 are shown in Fig. 2A. Growth was stimulated in a dose-dependent manner by E2 in all cell lines, while all cell lines showed growth inhibition by TS and low-dose of DHT (1 nM and 10 nM). Growth inhibition by 100 nM TS and 10 nM DHT in variant cell lines was significantly weaker than in the parental E10 cell line. In contrast to the parental E10 cell line, growth in the variant cell lines was stimulated by 100 nM DHT. All cell lines were stimulated by 3β-diol in a dose-dependent manner, but low-dose 3β-diol (1 nM or 10 nM) stimulated growth in the variant cell lines significantly more than in the parental E10 cell line.

The results of the ERE-luciferase reporter assay are shown in Fig. 2B. DHT 100 nM induced ER activity in variant, but not parental E10 cell lines. In addition, 100 nM 3β-diol-induced ER activities were two-fold higher in variant cell lines compared with the parental E10 cell lines. ER activity induced by DHT or 3β-diol was inhibited by 1 μM fulvestrant, but not by 100 nM letrozole.

The induction of estrogen- and androgen-responsive genes by TS, DHT and 3β-diol was analyzed using real-time PCR (Online Resource 5, Fig. S4). Variant cell lines showed increased induction of the estrogen-responsive genes for progesterone receptor, the transcription factor EGR3 [25] and Bcl2 by TS, DHT and 3β-diol, compared with the parental E10 cell line. In contrast, the androgen-responsive gene KLK3 [26] was induced by TS, DHT and 3β-diol in parental E10 cells, but not in variant cell lines.

These results indicate that the variant cell lines were adapted to androgen-abundant conditions and were hypersensitive to 3β-diol. It seems likely that this was the result of increased estrogenic, rather than androgenic functions of androgen and 3β-diol. These phenomena were also independent of aromatase activity.

Increased DHT metabolism and AR signal reduction might provide adaptability to androgen-abundant conditions

mRNA levels of androgen-producing and -metabolizing enzymes and hormone receptors in the variant and parental cells lines are shown in Fig. 3. Both variant lines (V1, V2) showed increased mRNA expression of HSD3B1 and reduced 5α-reductase type 1 and AR expression. AKR1C3 and ER were up-regulated in V2 cells. Aromatase (CYP19) and 17β-hydroxysteroid dehydrogenase type 2 were not detectable in any of the cell lines (data not shown). These results suggest that androgens may be metabolized more efficiently to 3β-diol (Online Resource 6, Fig. S5), which may exert estrogenic, rather than androgenic actions in variant cell lines, because of reduced androgen signal transduction.

In line with these hypotheses, HSD3B1-overexpressing E10 cells showed increased ER activity and growth stimulation by high-dose DHT (100 nM), in contrast to control E10 cells (Fig. 4A). Furthermore, the AR inhibitor bicalutamide reduced the inhibitory effect of DHT in E10 cells, and up-regulated their sensitivity to 3β-diol (Fig. 4B).

These results suggest that increased expression of HSD3B1 and decreased expression of AR may contribute to cell adaptation to androgen-abundant conditions, as demonstrated by the increased conversion of DHT to 3β-diol by HSD3B1 and AR signal reduction.

Variant cell lines were less sensitive to letrozole

We examined AI resistance in the variant cell lines using a coculture system to mimic local estrogen production from androgen in cancer tissues (Online Resource 4, Fig. S3). ER activities and cell growth were assessed under various conditions using this coculture system (Fig. 5). In coculture with stromal cells, 100 nM TS supplementation resulted in ER activation and growth stimulation in all cell lines, compared with untreated controls. ER activity in E10 cells induced by 100 nM TS was inhibited to untreated-control levels by 100 nM letrozole, while ER activity in variant cell lines was not completely inhibited. Cell growth of E10 cell lines induced by 100 nM TS supplementation was inhibited to less than that of untreated controls by 100 nM letrozole, while cell growth of the variant cell lines was unaffected by 100 nM TS- or 100 nM letrozole supplementation. The variant cell lines were therefore considered to be less sensitive to letrozole than the parental lines.

Discussion

In the present study, we successfully cloned two stable variant cell lines with androgen metabolite-dependent ER activity. Investigation of the process of adaptation to androgen-abundant conditions in these cell lines suggested that increased expression of HSD3B1 and reduced expression of AR might reduce the sensitivity of cells to AIs, as demonstrated by enhancement of androgen metabolite-induced ER activation and cell growth.

Although this model system had some limitations in replicating the endocrinology of postmenopausal women, the androgen-abundant and estrogen-depleted culture conditions reflected AI treatment conditions, rather than simple estrogen-depleted conditions. Even without AIs, these conditions were similar to AI treatment conditions in MCF-7 cells because of their low aromatase expression [27, 28]. We also confirmed that aromatase mRNA expression (CYP19) was not detectable in our E10 cells (data not shown).

As noted above, we aimed to establish clones based on a single mechanism, namely ER activation by androgen metabolites. We therefore used the E10 cell line to assess the ER activity of living cells and to select suitable clones. We subsequently obtained ER-dependent clones by assessing the ER activity of individual cells, and performed further screening to select clones that showed ER activity in an aromatase-independent and TS-dependent manner, excluding clones with constitutive ER activity, or clones in which ER activity was dependent on estrogens supplied by aromatase from TS. The V2 cell line showed relatively high ER activity in TS-depleted conditions, suggesting the possibility of ligand-independent ER activity.

Analysis of cell growth and ER activity induced by androgen or 3β-diol showed that variant cell lines were adapted for androgen-abundant conditions. Quantitative analysis of mRNA expression suggested that androgen or 3β-diol exerted estrogenic behavior independently of aromatase, as demonstrated by the increased conversion of DHT into 3β-diol and the reduced androgen signal in variant cell lines. These hypotheses support the idea that overexpression of HSD3B1 and inhibition of AR in E10 cells resulted in adaptation to estrogen-deprived and androgen-abundant conditions. A previous report showed that AR and ERα can interact directly and inhibit each other's transcriptional activity [29, 30]. Reduced AR expression may thus be one of the factors responsible for interrupting androgen signal transduction in variant cell lines.

Aromatase is highly expressed in the adipose stromal cells adjacent to the tumor in breast tumors [31, 32]. We previously reported that ERs were activated by coculture with adipose stromal cells isolated from breast tumor tissues in the presence of TS, as a substrate for aromatase [21]. The addition of TS alone had no effect on ER activity and an inhibitory effect on E10 cell growth, but TS induced ER activity and growth of E10 cells in a dose-dependent manner when cocultured with stromal cells, which effects were inhibited by 100 nM letrozole (data not shown). We used this coculture system to assess the inhibitory effect of AIs. AIs inhibit breast cancer cells by at least two separate mechanisms. They eliminate the growth-stimulating effect of estrogens by blocking estrogen production. ER activity induced by 100 nM TS in variant cell lines was not completely inhibited in this coculture system, suggesting that they might be the result of ER activation by androgen metabolites, including 3β-diol, produced in an aromatase-independent manner. The growth-inhibitory effect of androgens represents another possible mechanism. Androgens have been reported to have inhibitory effects in hormone-dependent breast cancer cells [4–6]. Luciana et al [9] found that cell growth was suppressed by low androgen levels in cells not supplemented by androgens and in conditions under which androgen cannot be converted to estrogen. Letrozole therefore exerted an extra effect beyond that produced by androgen supplementation in parental E10 cells. In contrast, established variant cell lines

showed letrozole-resistant ER activity and maintained their growth under TS- and letrozole-supplemented conditions in coculture with stromal cells. These results suggest that these cell lines were less sensitive to letrozole, because they showed both AR signal reduction and ER activation by androgen metabolites produced in an aromatase-independent manner.

It has been suggested that androgen metabolite-dependent ER activation and cell growth may play some roles in the mechanism of AI resistance. It is therefore necessary to investigate treatment strategies that will be effective against androgen metabolite-dependent ER activation and cell growth. 3β-Diol-induced growth in variant cell lines was inhibited by OHT, toremifene or fulvestrant, but not by AIs, suggesting a promising effect of SERMs on androgen metabolite-dependent growth mechanism (Online resource 7; Fig. S6). Sequential use of tamoxifen, toremifene or fulvestrant after first-line AIs has previously been suggested to be effective in patients with aromatase inhibitor-refractory advanced or metastatic breast cancer [33–36]. These findings might partly account for the efficacy of sequential use of SERMs or fulvestrant after first-line AIs.

We have initiated a clinical study to determine if androgen metabolite-dependent growth mechanisms are involved in AI-resistance in clinical breast cancer cases. Immunohistochemistry and real-time PCR analyses of nine pairs of primary and recurrent tissue samples from AI-resistant breast cancer revealed decreased AR protein expression in all cases, and increased HSD3B1 mRNA expression in five cases (data not shown). The significances of AR and HSD3B1 in clinical breast cancer are currently under further investigation.

In conclusion, we established new human breast cancer cell lines showing growth induction via ER activation by androgen metabolites. Characterization of these cell lines suggests that the androgen metabolite-dependent growth of hormone receptor-positive breast cancer may play a role in the mechanism of AI resistance.

Acknowledgments

We would like to thank Takashi Suzuki (Tohoku University Department of Pathology and Histotechnology) for discussions and helpful suggestions. This study was supported in part by a Grant-in-Aid for Scientific Research from the Ministry of Education, Culture, Sports, Science and Technology, Japan; a Grant-in-Aid for Cancer Research from the Ministry of Health, Labour and Welfare, Japan; the Program for Promotion of Fundamental Studies in Health Science of the National Institute of Biomedical Innovation (NIBIO); and a grant from the Smoking Research Foundation.

Ethical standards

All experiments complied with the current laws of Japan.

Conflict of Interest

The authors declare that they have no conflict of interest.

References

1. Chlebowski R, Cuzick J, Amakye D, Bauerfeind I, Buzdar A, Chia S, Cutuli B, Linforth R, Maass N, Noguchi S et al (2000) Clinical perspectives on the utility of aromatase inhibitors for the adjuvant

treatment of breast cancer. The Breast 18 Suppl 2: S1–11

2. Miller WR, Anderson TJ, Jack WJ (1990) Relationship between tumour aromatase activity, tumour characteristics and response to therapy. J Steroid Biochem Mol Biol 37:1055–1059
3. Sasano H, Miki Y, Nagasaki S, Suzuki T (2009) In situ estrogen production and its regulation in human breast carcinoma: from endocrinology to intracrinology. Pathol Int 59:777–789
4. Ortmann J, Prifti S, Bohlmann MK, Rehberger-Schneider S, Strowitzki T, Rabe T (2002) Testosterone and 5 alpha-dihydrotestosterone inhibit in vitro growth of human breast cancer cell lines. Gynecol Endocrinol 16:113–120
5. Andò S, De Amicis F, Rago V, Carpino A, Maggiolini M, Panno ML, Lanzino M (2002) Breast cancer: from estrogen to androgen receptor. Mol Cell Endocrinol 193:121–128
6. Labrie F, Luu-The V, Labrie C, Bélanger A, Simard J, Lin SX, Pelletier G (2003) Endocrine and intracrine sources of androgens in women: inhibition of breast cancer and other roles of androgens and their precursor dehydroepiandrosterone. Endocr Rev 24:152–182
7. Takagi K, Miki Y, Nagasaki S, Hirakawa H, Onodera Y, Akahira J, Ishida T, Watanabe M, Kimijima I, Hayashi S et al (2010) Increased intratumoral androgens in human breast carcinoma following aromatase inhibitor exemestane treatment. Endocr Relat Cancer 17:415–430
8. Hayashi S, Niwa T, Yamaguchi Y (2009) Estrogen signaling pathway and its imaging in human breast cancer. Cancer Sci 100:1773–1778
9. Macedo LF, Guo Z, Tilghman SL, Sabnis GJ, Qiu Y, Brodie A (2006) Role of androgens on MCF-7 breast cancer cell growth and on the inhibitory effect of letrozole. Cancer Res 66:7775–7782
10. Sabnis G, Brodie A (2010) Adaptive changes results in activation of alternate signaling pathways and resistance to aromatase inhibitor resistance. Mol Cell Endocrinol Epub Sep 16
11. Martin LA, Farmer I, Johnston SR, Ali S, Dowsett M (2005) Elevated ERK1 / ERK2 / estrogen receptor cross-talk enhances estrogen-mediated signaling during long-term estrogen deprivation. Endocr Relat Cancer 12 Suppl 1:S75–84
12. Yue W, Fan P, Wang J, Li Y, Santen RJ (2007) Mechanisms of acquired resistance to endocrine therapy in hormone-dependent breast cancer cells. J Steroid Biochem Mol Biol 106:102–110
13. Santen RJ, Song RX, Masamura S, Yue W, Fan P, Sogon T, Hayashi S, Nakachi K, Eguchi H (2008) Adaptation to estradiol deprivation causes up-regulation of growth factor pathways and hypersensitivity to estradiol in breast cancer cells. Adv Exp Med Biol 630:19–34
14. Fang H, Tong W, Branham WS, Moland CL, Dial SL, Hong H, Xie Q, Perkins R, Owens W, Sheehan DM (2003) Study of 202 natural, synthetic, and environmental chemicals for binding to the androgen receptor. Chem Res Toxicol 16:1338–1358
15. Steckelbroeck S, Jin Y, Gopishetty S, Oyesanmi B, Penning TM (2004) Human cytosolic 3 alpha-hydroxysteroid dehydrogenases of the aldo-keto reductase superfamily display significant 3 beta-hydroxysteroid dehydrogenase activity. J Biol Chem 279:10784–10795
16. Jin Y, Duan L, Lee SH, Kloosterboer HJ, Blair IA, Penning TM (2009) Human cytosolic hydroxysteroid dehydrogenases of the aldo-ketoreductase superfamily catalyze reduction of conjugated steroids. J Biol Chem 284:10013–10022
17. Lorence MC, Murry BA, Trant JM, Mason JI (1990) Human 3 beta-hydroxysteroid

dehydrogenase/delta 5→4isomerase from placenta: expression in nonsteroidogenic cells of a protein that catalyzes the dehydrogenation/isomerization of C21 and C19 steroids. Endocrinology 126:2493–2498

18. Wang P, Wen Y, Han G-Z, Sidhu PK, Zhu BT (2009) Characterization of the oestrogenic activity of non-aromatic steroids: are there male-specific endogenous oestrogen receptor modulators? Br J Pharmacol 158:1796–1807
19. Kuiper GG, Carlsson B, Grandien K, Enmark E, Häggblad J, Nilsson S, Gustafsson JA (1997) Comparison of the ligand binding specificity and transcript tissue distribution of estrogen receptors alpha and beta. Endocrinology 138:863–870
20. Sikora MJ, Cordero KE, Larios JM, Johnson MD, Lippman ME, Rae JM (2009) The androgen metabolite 5alpha-androstane-3beta,17beta-diol (3betaAdiol) induces breast cancer growth via estrogen receptor: implications for aromatase inhibitor resistance. Breast Cancer Res Treat 115:289–296
21. Yamaguchi Y, Takei H, Suemasu K, Kobayashi Y, Kurosumi M, Harada N, Hayashi S (2005) Tumor-stromal interaction through the estrogen-signaling pathway in human breast cancer. Cancer Res 65:4653–4662
22. Matsumoto M, Yamaguchi Y, Seino Y, Hatakeyama A, Takei H, Niikura H, Ito K, Suzuki T, Sasano H, Yaegashi N et al (2008) Estrogen signaling ability in human endometrial cancer through the cancer-stromal interaction. Endocr Relat Cancer 15:451–463
23. Omoto Y, Kobayashi Y, Nishida K, Tsuchiya E, Eguchi H, Nakagawa K, Ishikawa Y, Yamori T, Iwase H, Fujii Y et al (2001) Expression, function, and clinical implications of the estrogen receptor β in human lung cancers. Biochem Biophys Res Commun 285:340–347
24. Heneweer M, Muusse M, Dingemans M, de Jong PC, van den Berg M, Sanderson JT (2005) Co-culture of primary human mammary fibroblasts and MCF-7 cells as an in vitro breast cancer model. Toxicol Sci 83:257–263
25. Inoue A, Omoto Y, Yamaguchi Y, Kiyama R, Hayashi S (2004) Transcription factor EGR3 is involved in the estrogen-signaling pathway in breast cancer cell. J Mol Endocrinol 32:649–661
26. Lawrence MG, Lai J, Clements JA (2010) Kallikreins on steroids: structure, function, and hormonal regulation of prostate-specific antigen and the extended kallikrein locus. Endocr Rev 31:407–446.
27. Santner SJ, Chen S, Zhou D, Korsunsky Z, Martel J, Santen RJ (1993) Effect of androstenedione on growth of untransfected and aromatase-transfected MCF-7 cells in culture. J Steroid Biochem Mol Biol 44:611–616
28. Sasano H, Ozaki M (1997) Aromatase expression and its localization in human breast cancer. J Steroid Biochem Mol Biol 61:293–298
29. Panet-Raymond V, Gottlieb B, Beitel LK, Pinsky L, Trifiro MA (2000) Interactions between androgen and estrogen receptors and the effects on their transactivational properties. Mol Cell Endocrinol 167:139–150
30. Peters AA, Buchanan G, Ricciardelli C, Bianco-Miotto T, Centenera MM, Harris JM, Jindal S, Segara D, Jia L, Moore NL et al (2009) Androgen receptor inhibits estrogen receptor-alpha activity and is prognostic in breast cancer. Cancer Res 69:6131–6140

31. O'Neill JS, Miller WR (1987) Aromatase activity in breast adipose tissue from women with benign and malignant breast disease. Br J Cancer 56:601–604
32. Santen RJ, Santner SJ, Pauley RJ, Tait L, Kaseta J, Demers LM, Hamilton C, Yue W, Wang JP (1997) Estrogen production via the aromatase enzyme in breast carcinoma: which cell type is responsible? J Steroid Biochem Mol Biol 61:267–271
33. Thürlimann B, Robertson JF, Nabholtz JM, Buzdar A, Bonneterre J, Arimidex Study Group (2003) Efficacy of tamoxifen following anastrozole ('Arimidex') compared with anastrozole following tamoxifen as first-line treatment for advanced breast cancer in postmenopausal women. Eur J Cancer 39:2310–2317
34. Koyama H, Iesato A, Fukushima Y, Okada T, Watanabe T, Harada M, Ito T, Maeno K, Mochizuki Y, Ito K et al (2011) A retrospective study of high-dose toremifene treatment for patients with aromatase inhibitor refractory advanced or metastatic hormone receptor-positive breast cancer. Gan To Kagaku Ryoho 38:1123–1126 [In Japanese]
35. Yamamoto Y, Masuda N, Ohtake T, Yamashita H, Saji S, Kimijima I, Kasahara Y, Ishikawa T, Sawaki M, Hozumi Y et al (2010) Clinical usefulness of high-dose toremifene in patients relapsed on treatment with an aromatase inhibitor. Breast Cancer 17:254–260
36. Chia S, Gradishar W, Mauriac L, Bines J, Amant F, Federico M, Fein L, Romieu G, Buzdar A, Robertson JF et al (2008) Double-blind, randomized placebo controlled trial of fulvestrant compared with exemestane after prior nonsteroidal aromatase inhibitor therapy in postmenopausal women with hormone receptor-positive, advanced breast cancer: results from EFECT. J Clin Oncol 26:1664–1670

Figure Legends

Fig. 1 Screening of variant cells

After 3 months of culture in TS-supplemented steroid-depleted medium, five clones expressing GFP were selected. ER activities were assessed in a single experiment as the proportion of GFP-positive cells at each step

Fig. 2 Steroid-induced growth and ER activity of cell lines

a Steroid-induced growth of E10 and variant cell lines. Cells were plated in 24-well culture plates at a density of 10,000 cells/well with steroid-depleted medium, after 3 days of incubation in steroid-depleted medium. The indicated concentrations of E2, TS, DHT, 3β-diol or vehicle control (EtOH) were added to each well for 4 days. Cells from each well were then harvested and counted. Value relative to the vehicle control is shown. All data are shown as mean ± SD of three independent experiments (*$P < 0.05$). **b** ER activity of variant cell lines induced by androgen or 3β-diol. After 3 days of incubation in steroid-depleted medium, each cell line was plated on culture plates in the same medium and incubated for 48 h. Each cell line was then cotransfected with the ERE-luciferase reporter and the pRL-luciferase plasmid as a control. Luciferase activities were assayed after culturing for a further 24 h in the presence of 100 nM TS, DHT, 3β-diol, 10 nM E2, with or without 100 nM letrozole or 1 μM fulvestrant. All data shown are mean ± SD of three independent experiments (*$P < 0.05$)

Fig. 3 mRNA expression of androgen-metabolizing enzymes and steroid receptors in E10 and variant cell lines

Total RNA was extracted from each cell line cultured in regular growth medium (Normal) or steroid-depleted medium supplemented with 100 nM TS (TS) for at least 3 days. All PCRs were performed in duplicate, and the expression of the target gene relative to RPL13A as an internal control is shown (mean ± SD)

Fig. 4 Effects of HSD3B1 over-expression and androgen receptor inhibitor in E10 cells

a Steroid-induced growth of E10 cells transfected with HSD3B1 expression vector. Cells that were transfected with HSD3B1 expression vector (E10-HSD3B1) or control vector (E10-Control) were generated as described in Materials and methods. After 3 days of incubation in steroid-depleted medium, each cell line was plated on culture plates in the same medium and incubated for 48 h. Each cell line was then cotransfected with the ERE-luciferase reporter and the pRL-luciferase plasmid as a control. Luciferase activities were assayed after culturing for a further 24 h in the presence of 100 nM DHT or vehicle control (EtOH). The value relative to the vehicle control is shown. All data are shown as mean ± SD of three independent experiments (left graph). After 3 days of culture in steroid-depleted medium, these cells were plated in 24-well culture plates at a density of 10,000 cells/well with steroid-depleted medium. The indicated concentrations of DHT or the vehicle control (EtOH) were added to each well for 4 days. Cells from each well were then harvested and counted. Values relative to the vehicle control are shown (right graph). All data shown are mean ± SD of three independent experiments. **b** Effect of androgen receptor inhibitor bicalutamide in parental E10 cell line. After 3 days of culture in steroid-depleted medium, E10 cells were plated in 24-well culture plates at a density of 10,000 cells/well in steroid-depleted medium. The indicated concentrations of DHT, 3β-diol or vehicle control (EtOH), with or without bicalutamide (10 μM), were added to each well for 4

days. Cells from each well were then harvested and counted. Values relative to the vehicle control are shown. All data shown are mean ± SD of three independent experiments

Fig. 5 Cell growth and ERE-GFP reporter assays in coculture with primary stromal cells
After 3 days of incubation in steroid-depleted medium, cancer cell lines and stromal cells were plated in the bottom of wells of a 24-well culture plate with an insert layer as described in Materials and methods. The cells were then incubated for 4 days with or without 100 nM TS and 100 nM letrozole before cell growth and ERE-GFP reporter assays. Cancer cells at the bottom of each well were washed, harvested and counted. ER activity of cancer cells in coculture was also assessed by counting the proportion of GFP-positive cells in the well bottom. The values relative to that of the vehicle control are shown. All data shown are mean ± SD of three independent experiments (*$P < 0.05$). Let, letrozole

Fig. S1 Establishment of E10 cells and screening of variant cell lines
a E10 cells report ER activity via GFP expression. ERE-tk-GFP-MCF-7 cells (E10 cells) were established from the human breast cancer cell line, MCF-7, by introduction of a plasmid carrying the ERE fused with ERE-GFP gene. These cells show luminescence via GFP, corresponding to ER transcription activity. **b** Screening of variant cell lines that show ER activity depending on androgen metabolites. We used E10 cells to establish variant cell lines. After 3 months of culture in TS-supplemented steroid-depleted medium, five clones expressing GFP (representing ER activity) were obtained. ER activities at each step of treatment (a, b, c, d, e) were assessed in a single experiment, as described in Materials and methods. E, estrogen; Let, letrozole; Ful, fulvestrant

Fig. S2 Expression of HSD3B1 in E10-HSD3B1 cells
Cells transfected with HSD3B1 expression vector (E10-HSD3B1) or control vector (E10-Control) were generated as described in Materials and methods. The expression level of HSD3B1 under regular growth medium was analyzed using real-time PCR. Values relative to RPL13A are shown

Fig. S3 Interaction coculture system using insert layers
To assess the inhibitory effect of AIs in E10 and variant cell lines, we used interaction cultures, defined as cocultures where cancer cells and stromal cells are grown separated by a membrane, but are allowed to interact via soluble factors, and have the same microenvironment, such as local estrogen synthesis from androgen by aromatase in stromal cells

Fig. S4 Induction of estrogen- or androgen-responsive genes by androgen or 3β-diol
After 3 days of incubation in steroid-depleted medium, 100 nM TS, DHT, 3β-diol or vehicle control (EtOH) was added to each cell line for 4 days before total RNA extraction. Total RNA was extracted from each cell line cultured in the indicated culture conditions, and real-time PCRs for expression of the indicated mRNA were carried out as described in Materials and methods. All PCRs were performed in duplicate, and the expression of the target gene relative to vehicle control is shown (mean ± SD)

Fig. S5 Estrogen synthesis and androgen metabolism

In postmenopausal women, estrogens are mainly supplied by aromatase from androgens (TS and androstenedione) biosynthesized in the adrenal gland. In contrast, 5α-androstane-3β,17β-diol (3β-diol) is generated from DHT by HSD3B1 type 1 and AKR1C3. It was suggested that the metabolizing pathway from DHT to 3β-diol is up-regulated in variant cell lines

Fig. S6 Blockage of 3β-diol-induced growth in variant cell lines by SERMs

After 3 days of culture in steroid-depleted medium, each cell line was plated in 24-well culture plates at a density of 10,000 cells/well in steroid-depleted medium. A volume of 100 nM 3β-diol or vehicle control (EtOH), with or without 1 μM OHT, 3 μM toremifene (TOR), 1 μM fulvestrant (Ful), 100 nM letrozole (Let), 100 nM anastrozole (Ana) or 100 nM exemestane (Exe), was added to each well for 4 days. Cells from each well were then harvested and counted. Values relative to the vehicle control are shown. All data are shown as mean ± SD of three independent experiments

Fig. 1

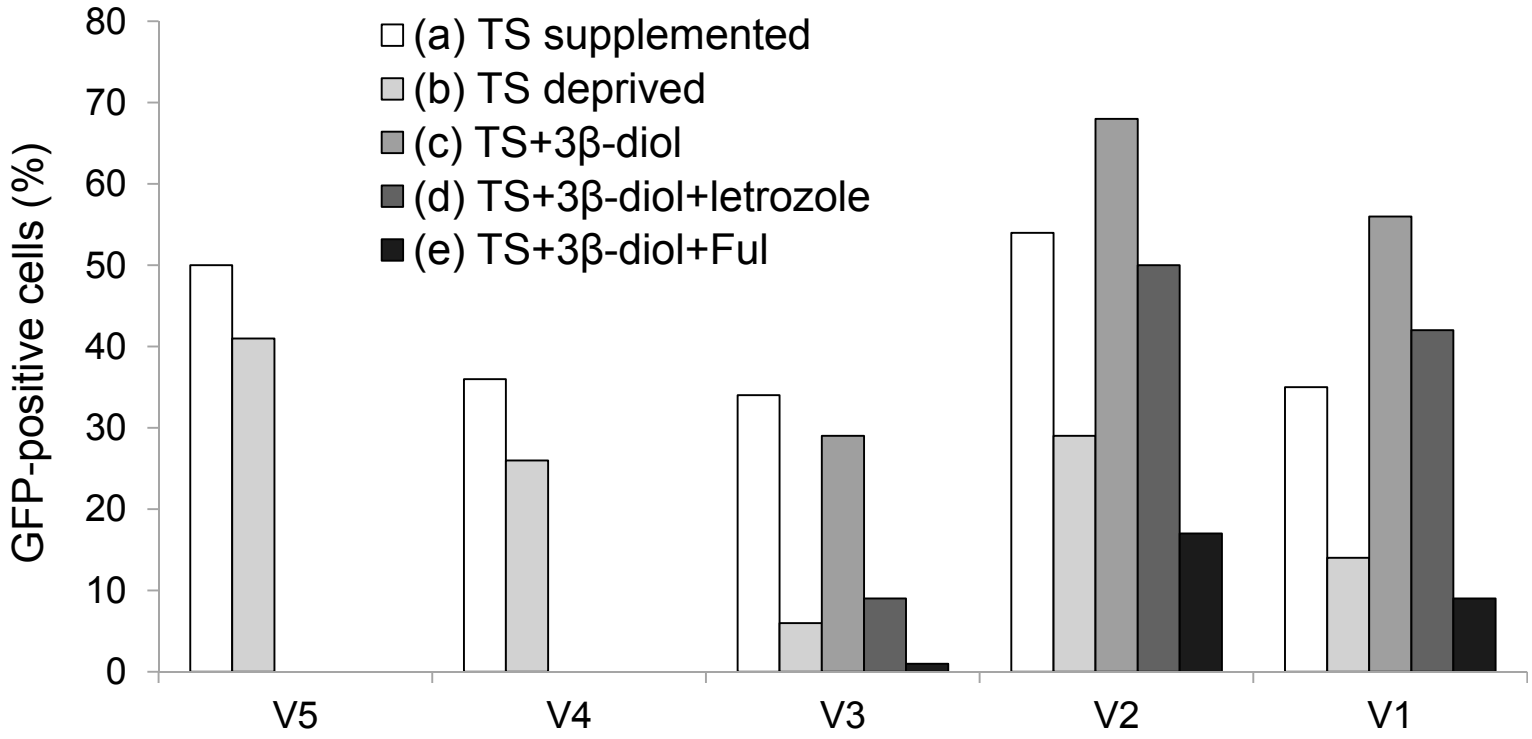
80
70
60
50
40
30
20
10
0
GFP-positive cells (%)
(a) TS supplemented
(b) TS deprived
(c) TS+3β-diol
(d) TS+3β-diol+letrozole
(e) TS+3β-diol+Ful
V5
V4
V3
V2
V1

Fig. 2

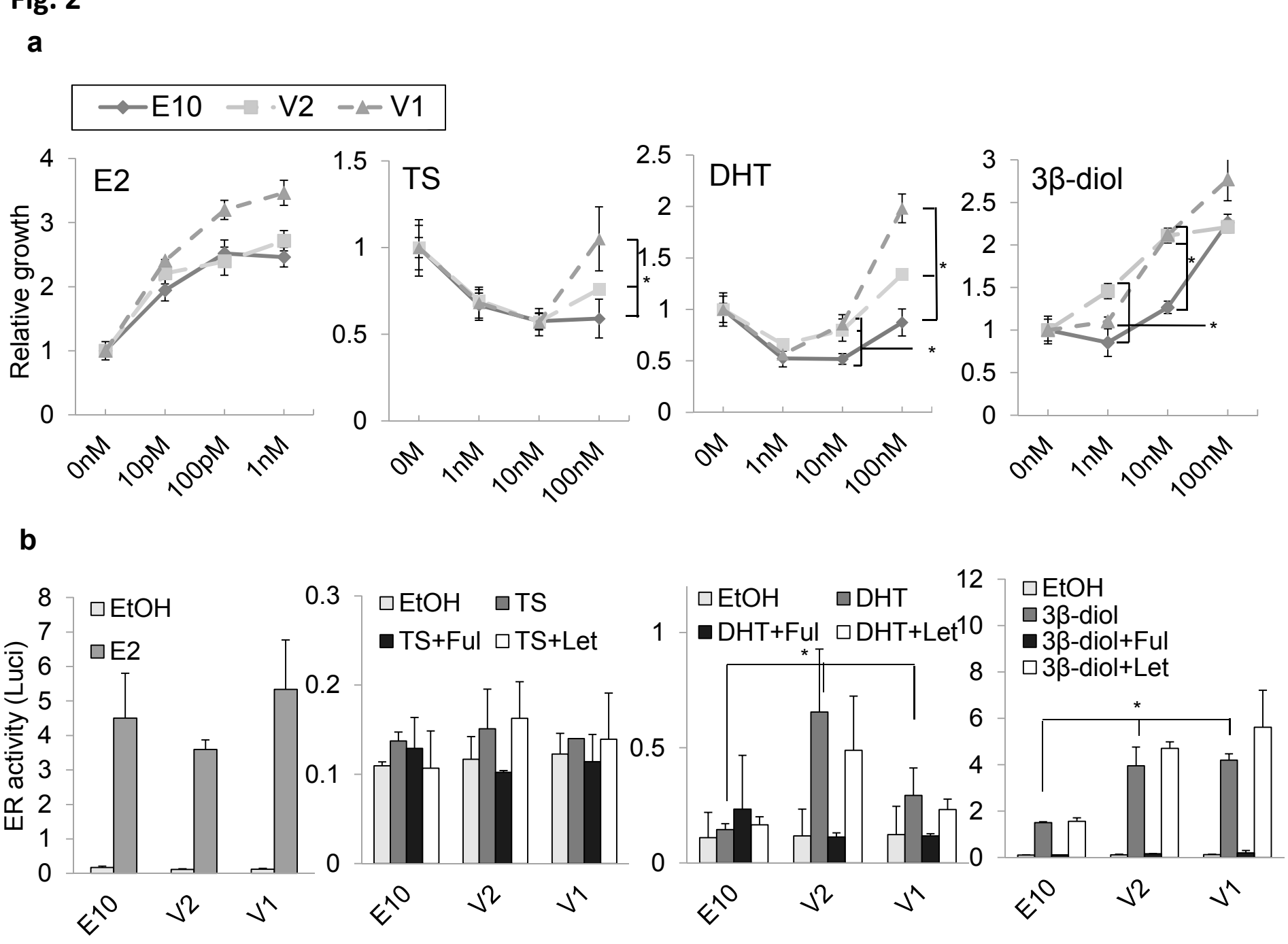
a
E10
V2
V1
E2
TS
DHT
3β-diol
Relative growth
0nM
10pM
100pM
1nM
0M
1nM
10nM
100nM
*
b
EtOH
E2
TS
TS+Ful
TS+Let
DHT
DHT+Ful
DHT+Let
3β-diol
3β-diol+Ful
3β-diol+Let
ER activity (Luci)
E10
V2
V1

Fig. 3

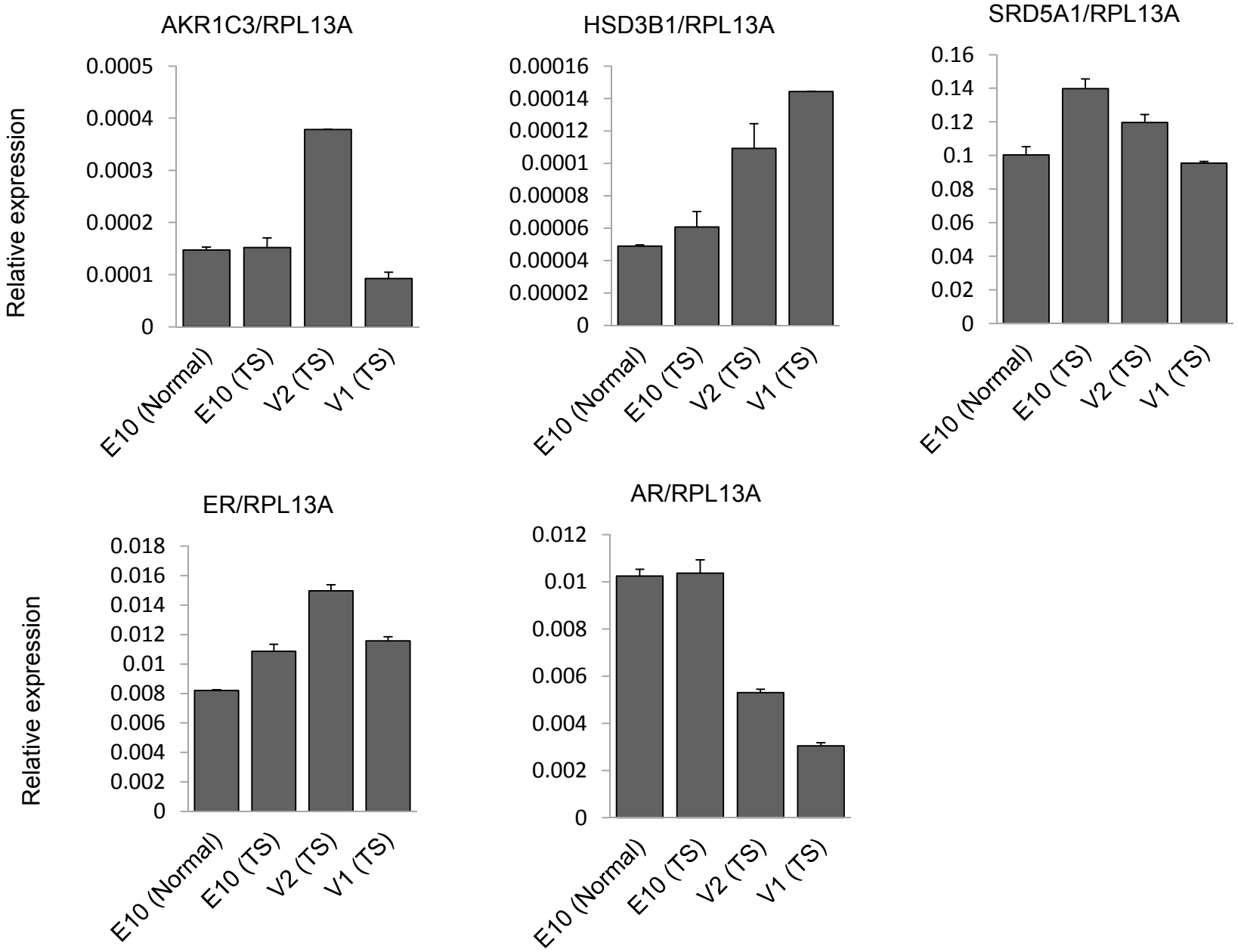
AKR1C3/RPL13A
HSD3B1/RPL13A
SRD5A1/RPL13A
ER/RPL13A
AR/RPL13A
Relative expression
Relative expression
0.0005
0.0004
0.0003
0.0002
0.0001
0
0.00016
0.00014
0.00012
0.0001
0.00008
0.00006
0.00004
0.00002
0
0.16
0.14
0.12
0.1
0.08
0.06
0.04
0.02
0
0.018
0.016
0.014
0.012
0.01
0.008
0.006
0.004
0.002
0
0.012
0.01
0.008
0.006
0.004
0.002
0
E10 (Normal)
E10 (TS)
V2 (TS)
V1 (TS)

Fig. 4

a

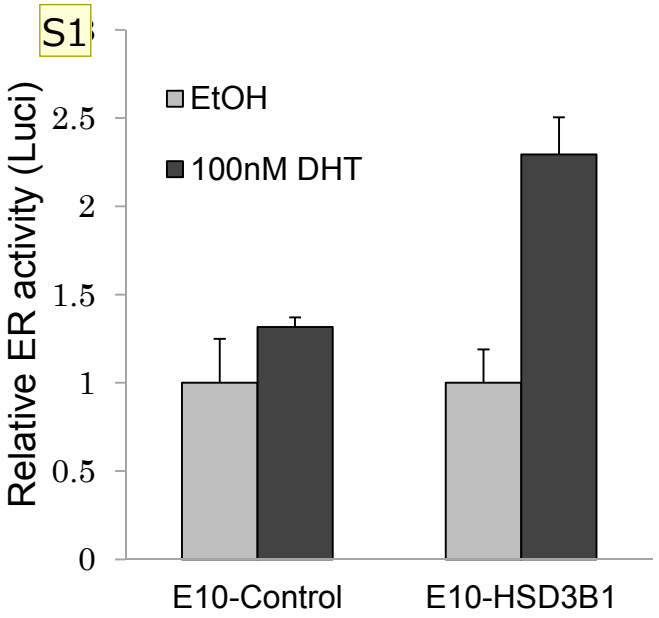
S1
EtOH
100nM DHT
Relative ER activity (Luci)
2.5
2
1.5
1
0.5
0
E10-Control
E10-HSD3B1

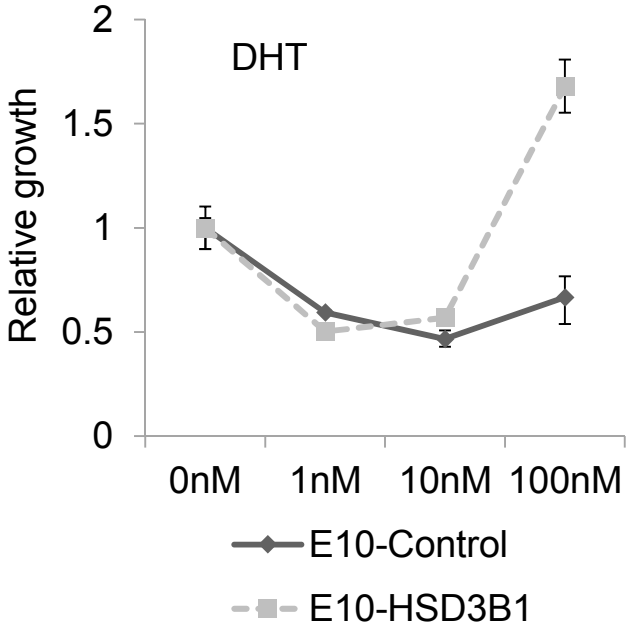
DHT
Relative growth
2
1.5
1
0.5
0
0nM
1nM
10nM
100nM
E10-Control
E10-HSD3B1

b

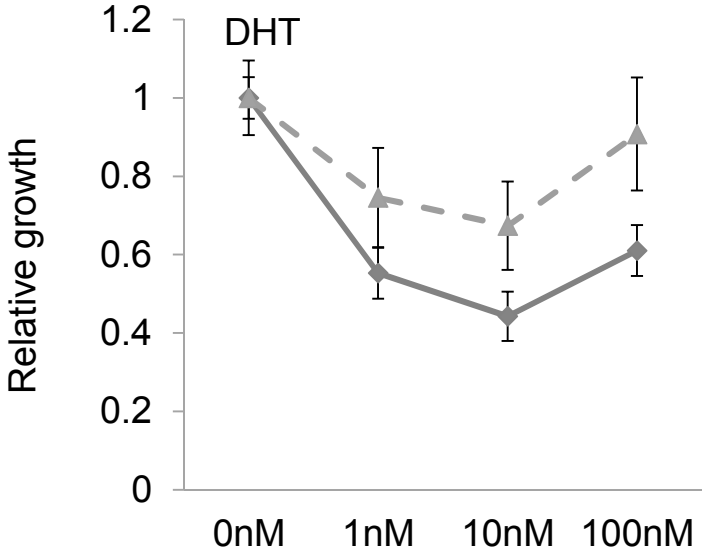
DHT
Relative growth
1.2
1
0.8
0.6
0.4
0.2
0
0nM
1nM
10nM
100nM

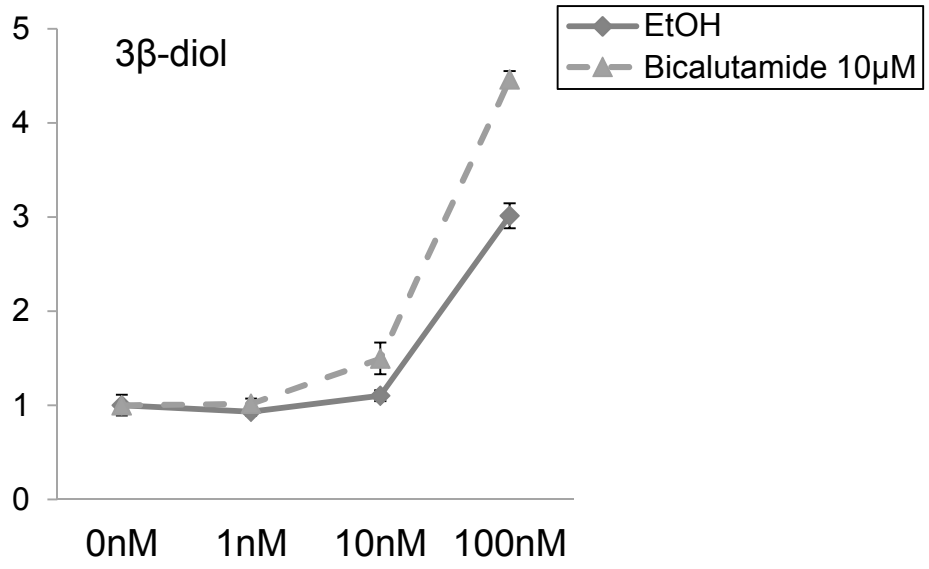
3β-diol
EtOH
Bicalutamide 10μM
5
4
3
2
1
0
0nM
1nM
10nM
100nM

Fig. 5

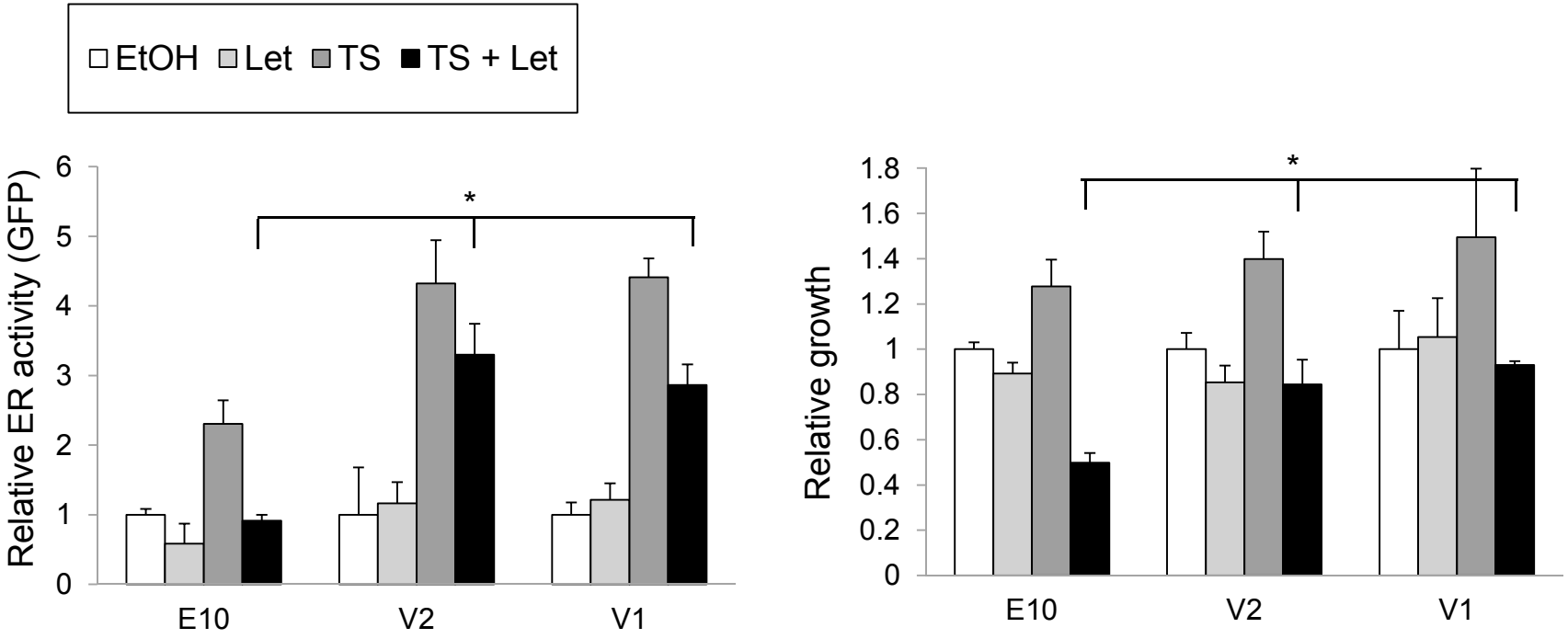
EtOH
Let
TS
TS + Let
Relative ER activity (GFP)
0
1
2
3
4
5
6
*
E10
V2
V1
Relative growth
0
0.2
0.4
0.6
0.8
1
1.2
1.4
1.6
1.8
*
E10
V2
V1

Fig. S1

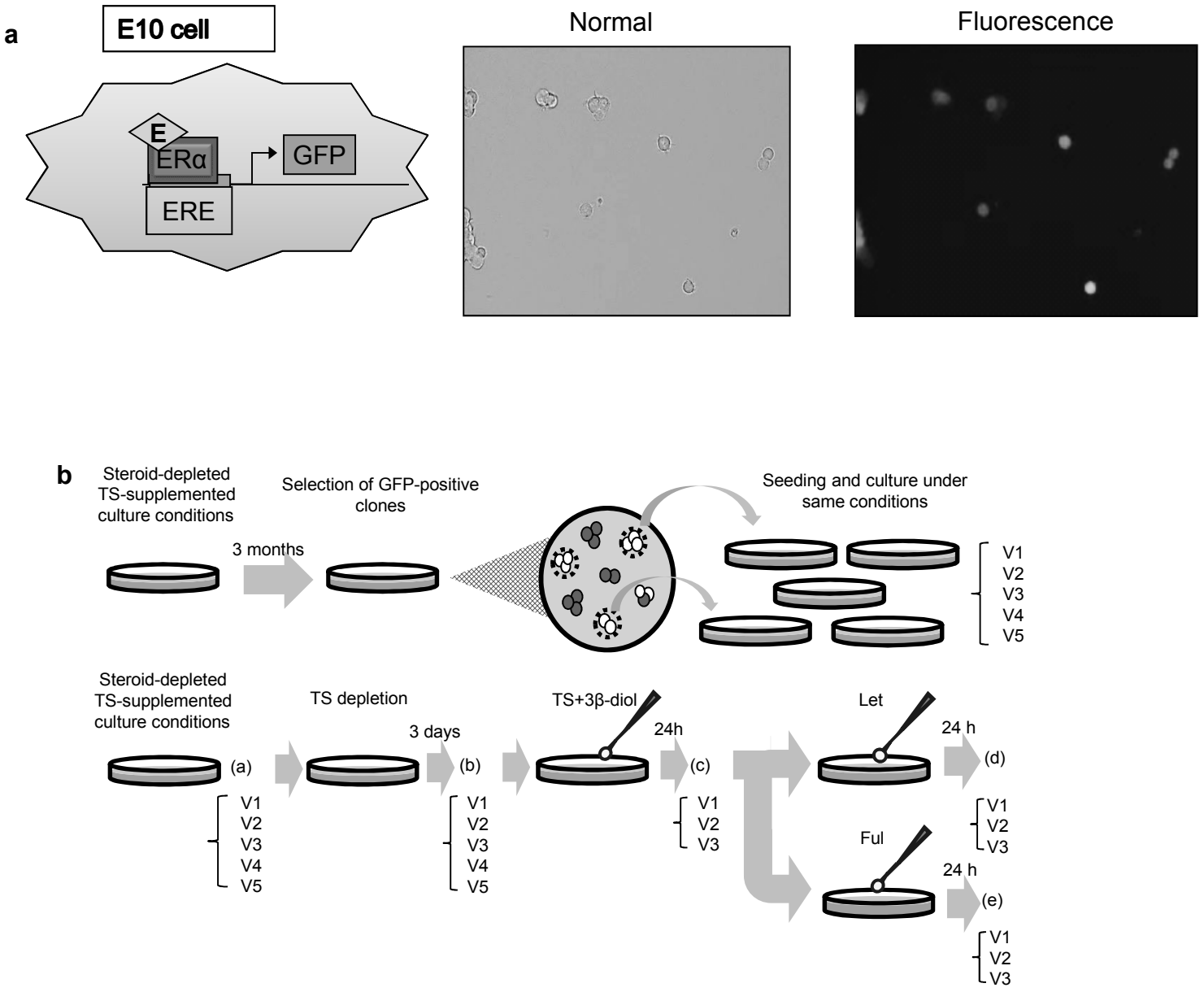
a
E10 cell
E
ERα
GFP
ERE
Normal
Fluorescence
b
Steroid-depleted TS-supplemented culture conditions
3 months
Selection of GFP-positive clones
Seeding and culture under same conditions
V1
V2
V3
V4
V5
Steroid-depleted TS-supplemented culture conditions
(a)
TS depletion
3 days
(b)
TS+3β-diol
24h
(c)
Let
24 h
(d)
Ful
24 h
(e)

Table S1 Primers used for real-time PCR analysis

Target mRNA	Accession number	Sequence	Final (nM)	Product (bp)
RPL13A	NM_012423.3	forward, 5’-CCT GGA GGA GAA GAG GAA AG-3’	500	126
		reverse, 5’-TTG AGG ACC TCT GTG TAT TT-3’	500	
SRD5A1	NM_001047.2	forward, 5’-CAA GGG GAG GCT TAT TTG AA-3	500	115
		reverse, 5’-TCA TGA TGC TCT TTT GCT CTA C-3’	500	
AKR1C3	NM_003739.4	forward, 5’-GCC TAG ACA GAA ATC TCC AC-3’	500	110
		reverse, 5’-TCT GGT AGA CAT CAG GCA AA-3’	500	
HSD3B1	NM_000862.2	forward, 5’-GAA AGG TAC CCA GCT CCT GTT A-3’	500	244
		reverse, 5’-ACA AGT GTA CAG GGT GCC G-3’	500	
CYP19	NM_031226.2	forward 5'-CCT TCT GCG TCG TGT CAT GCT-3'	300	116
		reverse 5'-GGA GAG CTT GCC ATG CAT CAA-3'	300	
HSD17B2	NM_002153.2	forward 5'-GCG GCT GTG ACC ATG TTC T-3'	500	115
		reverse 5'-TGT CAC TGG TGC CTG CGA T-3'	500	
ERα	NM_000125.3	forward, 5'-CTC CCA CAT CAG GCA CAT-3'	500	94
		reverse, 5'-CTC CAG CAG CAG GTC ATA-3'	500	
AR	NM_000044.3	forward, 5’-ATG TGG AAG CTG CAA GGT CT-3’	300	126
		reverse, 5’-CGA AGA CGA CAA GAT GGA CA-3’	300	

PgR	NM_000926.4	forward, 5’-AGC TCA CAG CGT TTC TAT CA-3'	500	101
		reverse, 5'-CGG GAC TGG ATA AAT GTA TTC-3'	500	
EGR3	NM_004430.2	forward, 5'-GAG CAG TTT GCT AAA CCA AC-3'	500	138
		reverse, 5'-AGA CCG ATG TCC ATT ACA TT-3'	500	
KLK3	NM_001648.2	forward, 5'-TGT CCG TGA CGT GGA TT-3'	200	107
		reverse, 5'-ACG AGA GGC CAC AAG CA-3'	200	
Bcl-2	NM_000633.2	forward, 5'-GTG GAT GAC TGA GTA CCT GAA C-3'	300	119
		reverse, 5'-GCC AGG AGA AAT CAA ACA-3'	300	

Fig. S2

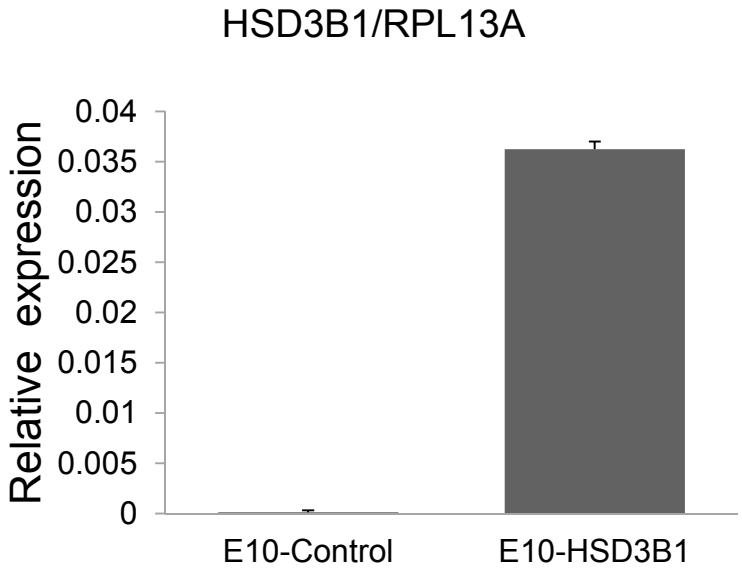
HSD3B1/RPL13A
Relative expression
0.04
0.035
0.03
0.025
0.02
0.015
0.01
0.005
0
E10-Control
E10-HSD3B1

Fig. S3

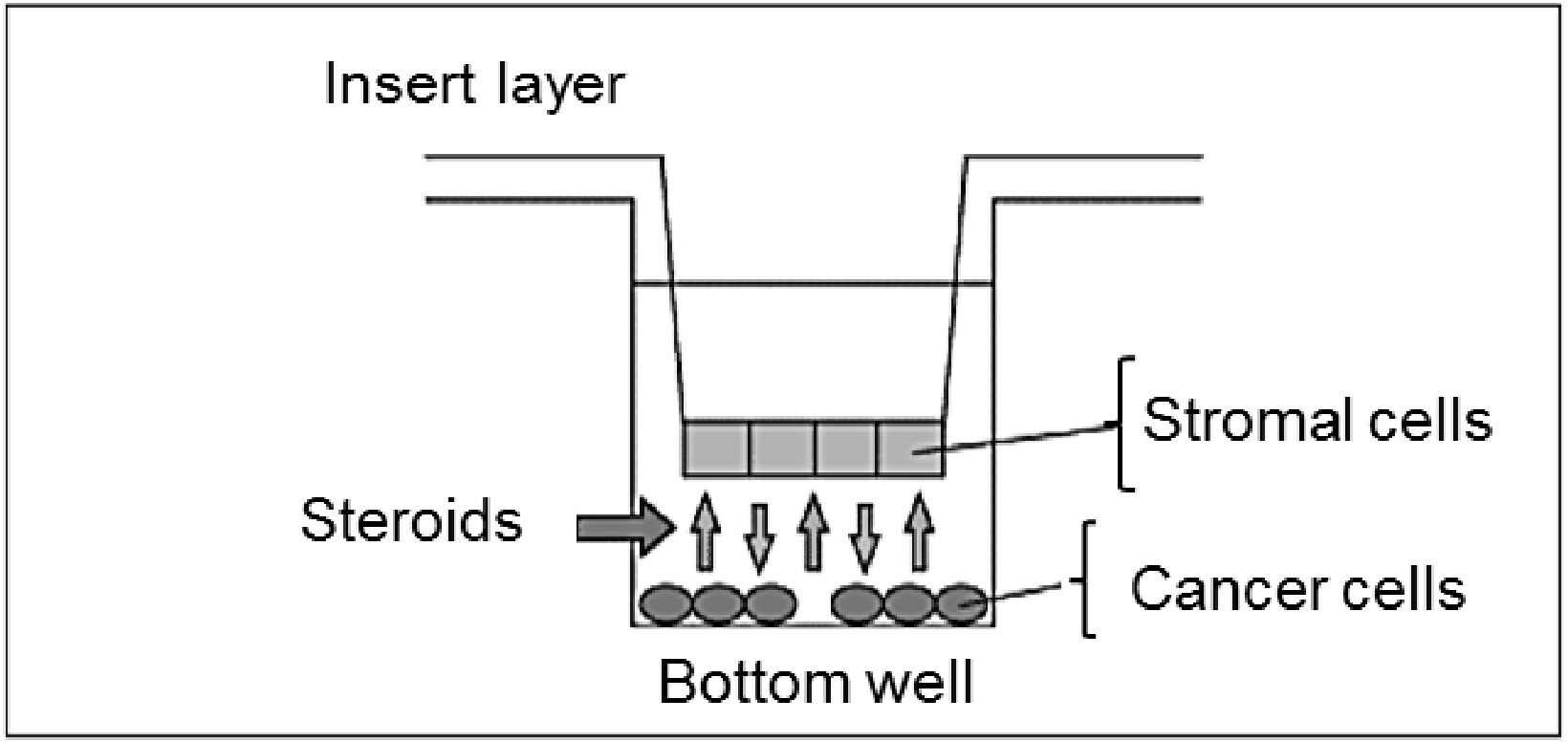
Insert layer
Stromal cells
Steroids
Cancer cells
Bottom well

Fig. S4

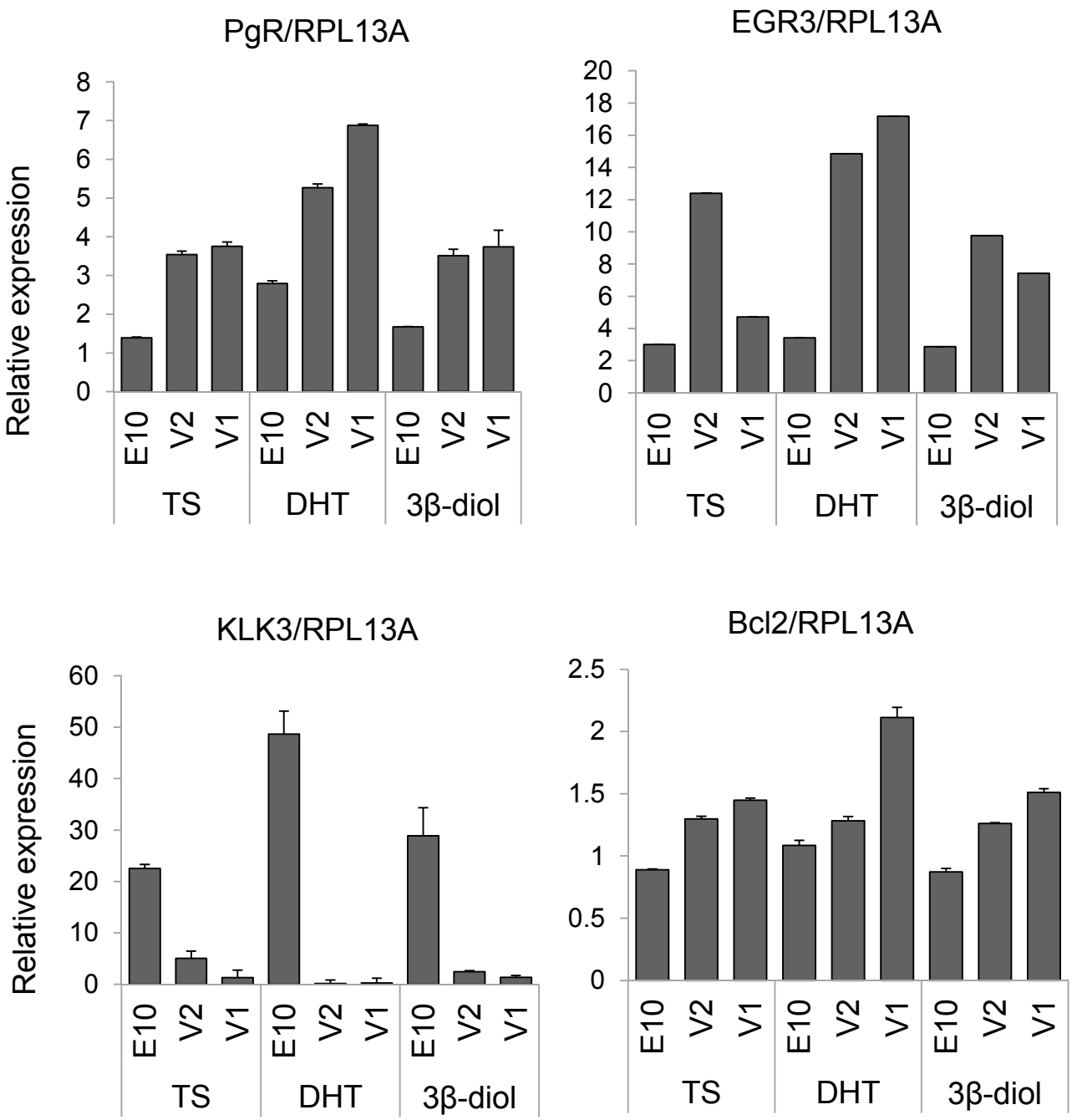
PgR/RPL13A
EGR3/RPL13A
KLK3/RPL13A
Bcl2/RPL13A
Relative expression
E10
V2
V1
TS
DHT
3β-diol

Fig. S5

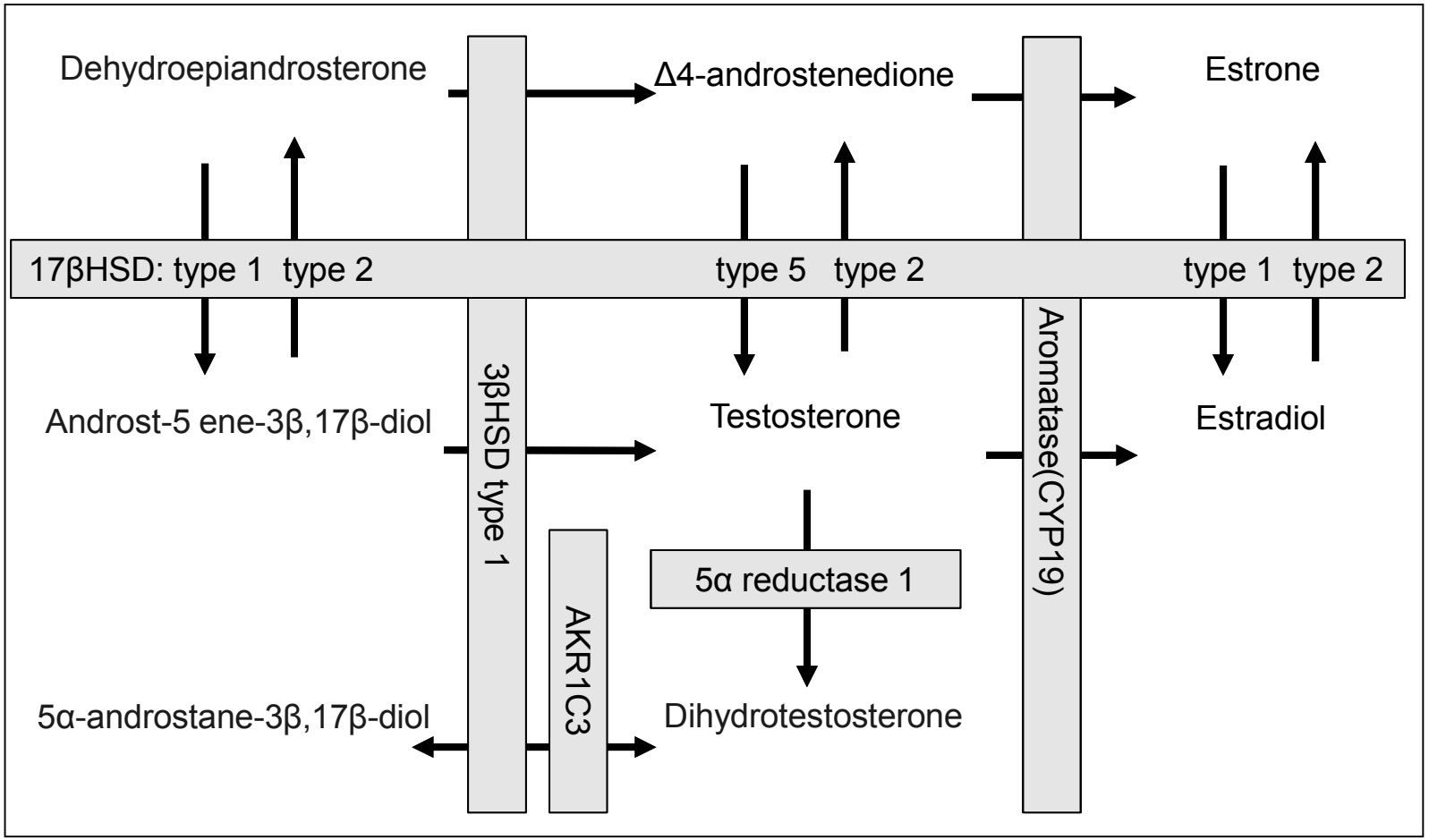
Dehydroepiandrosterone
Δ4-androstenedione
Estrone
17βHSD: type 1
type 2
type 5
type 2
type 1
type 2
Androst-5 ene-3β,17β-diol
3βHSD type 1
Testosterone
Aromatase(CYP19)
Estradiol
5α reductase 1
AKR1C3
5α-androstane-3β,17β-diol
Dihydrotestosterone

Fig. S6

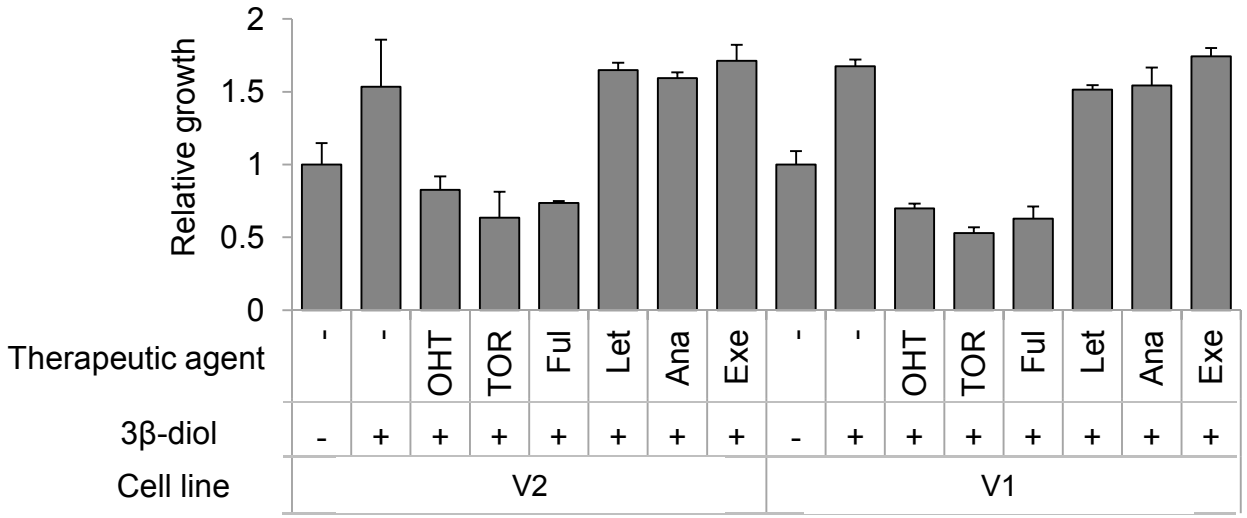
Relative growth
2
1.5
1
0.5
0
Therapeutic agent
-
-
OHT
TOR
Ful
Let
Ana
Exe
-
-
OHT
TOR
Ful
Let
Ana
Exe
3β-diol
-
+
+
+
+
+
+
+
-
+
+
+
+
+
+
+
Cell line
V2
V1